



ELSEVIER

Applied Catalysis A: General 125 (1995) 233–245



# Synthesis of tin-silicalite molecular sieves with MEL structure and their catalytic activity in oxidation reactions

Nawal Kishor Mal, Veda Ramaswamy, S. Ganapathy,  
A.V. Ramaswamy \*

*National Chemical Laboratory, Pune 411008, India*

Received 3 August 1994; revised 17 November 1994; accepted 13 January 1995

---

## Abstract

Tin-containing, medium pore molecular sieves (Si/Sn ratios above 40) with MEL structure have been synthesized hydrothermally and characterized by a variety of techniques. Changes in unit cell volume (XRD) account for about 20% of Sn<sup>4+</sup> ions in possible tetrahedral positions. <sup>119</sup>Sn MAS-NMR spectra, however, indicate that these are mostly in octahedral coordination. Framework IR spectra show an absorption at 970 cm<sup>-1</sup> which is associated with Si–O–Sn vibration. Despite the uncertainty of the environment of the Sn<sup>4+</sup> ions in the silicalite structure, these tin-silicates are found to be quite active in the hydroxylation of phenol and toluene with aqueous H<sub>2</sub>O<sub>2</sub> as oxidant. The product distribution suggests that most of the Sn<sup>4+</sup> ions are located within the channels of the MEL structure.

*Keywords:* Tin-silicates; Tin-MEL-silicalites; Sn-silicates synthesis; Hydroxylation on Sn-silicates; Oxidation with H<sub>2</sub>O<sub>2</sub> on Sn-silicates

---

## 1. Introduction

The possibility of isomorphous substitution of tin for aluminium in the framework of a number of zeolites such as faujasites, mordenite, ZSM-5, zeolite L and omega either by post-synthesis procedures [1–4] or by hydrothermal synthesis [5,6] is suggested in the literature but has not been confirmed. Exxon has claimed recently the synthesis of stannosilicates of novel structures in presence of alkali metals and Al or Ga, where Sn<sup>4+</sup> ions are reportedly octahedrally coordinated [6].

---

\* Corresponding author. E-mail: avr@ncl.ernet.in, fax. (+91-212) 334761.

Substitution of tin in molecular sieve zeolites is expected to impart certain properties which are useful in their application as adsorbents [6], as ionic conductors [7,8] and as catalysts in several hydrocarbon conversion processes [1–4]. Substitution of  $\text{Sn}^{\text{IV}}$  for  $\text{P}^{\text{V}}$  in the  $\text{AlPO}_4\text{-5}$  structure, for instance, is shown to generate Brønsted and Lewis acid sites [9]. Substitution of Si by Sn is not reported in the literature unless a trivalent element (e.g.,  $\text{Al}^{3+}$ ) is present in the framework. In the case of Al-free MFI, only a few studies have clearly evidenced the incorporation of another tetravalent element like  $\text{Ti}^{4+}$  [10] and  $\text{Ge}^{4+}$  [11]. We have recently communicated the synthesis of Sn-containing silicalite-1 (MFI structure) and shown that some of the  $\text{Sn}^{4+}$  ions may be in the framework positions [12]. Here, we present our findings on the synthesis of Sn-MEL silicates, their characterization by XRD, adsorption, IR and  $^{29}\text{Si}$  and  $^{119}\text{Sn}$  NMR spectroscopy and their potential as catalysts (like the titanium silicalites) in the oxidation of phenol and toluene using aqueous  $\text{H}_2\text{O}_2$  as oxidant.

## 2. Experimental

### 2.1. Synthesis

The hydrothermal synthesis of Al-free tin-silicates was carried out using gels of the following molar compositions:  $1.0 \text{ SiO}_2 : x \text{ SnO}_2 : 0.40 \text{ TBAOH} : 30 \text{ H}_2\text{O}$ , where  $x = 0.005$  to  $0.025$  and TBAOH ( $\text{Bu}_4\text{NOH}$ ) is the organic template. In a typical synthesis, 0.52 g of  $\text{SnCl}_4 \cdot 5\text{H}_2\text{O}$  (Loba Chemie, 99%) was added to a solution of 15.3 g of tetraethyl orthosilicate (TEOS) (Aldrich, 98%) under stirring. After 15 min, 18.7 g of TBAOH (40% aqueous solution, Aldrich) was added under vigorous stirring. This mixture was stirred for 1 h and 27.7 g of water was then added to the resultant clear solution and stirred for another 30 min. The homogeneous reaction mixture was charged into a stainless steel autoclave and heated at 433 K for 60 h for the crystallization to complete. After crystallization, the product was filtered, washed with deionised water, dried at 383 K and calcined at 773 K. The product yield was between 70 and 80 mass percentage. Four such Sn-silicalite-2 samples (Sn-Sil-2) with Si/Sn ratios of 40, 50, 70, and 100 were prepared. For comparison, a silicalite-2 (Sil-2) sample and a Sn-impregnated silicalite-2 sample were prepared. The latter was made by impregnating Sil-2 with  $\text{SnCl}_4$  solution and then calcining at 773 K. An amorphous Sn-silica sample (Si/Sn = 70) was also prepared from the gel obtained by mixing thoroughly under stirring a solution of  $\text{SnCl}_4 \cdot 5\text{H}_2\text{O}$  with TEOS, drying, washing and calcining the resultant material at 773 K.

### 2.2. Characterization

Both AAS (Hitachi) and ICP (John Yvon JYU-38 VHR) instruments were used for wet chemical analysis of the samples. The Si/Sn ratios of the calcined samples were obtained by XRF (Rigaku, model 3070) technique.

The crystallinity and phase purity of the samples were checked from the X-ray diffraction profiles recorded in a Rigaku (model D Max III VC, Ni-filtered Cu K $\alpha$  radiation and graphite monochromator) instrument in relation to the data reported by Fyfe et al. [13] for the MEL silicalite-2 sample. Silicon was used as internal standard for unit cell calculations at a scan rate of 0.25° 2 $\theta$  min<sup>-1</sup>. The lattice parameters were refined using a least square fit.

The sorption measurements for H<sub>2</sub>O, n-hexane and cyclohexane were carried out gravimetrically in a (Cahn, 2000G model) electrobalance at 298 K and at a fixed  $p/p_0$  of 0.5 after equilibration for 3 h. The surface areas and the micropore volumes were calculated from the N<sub>2</sub> adsorption isotherms at partial pressures of less than 0.1 using a Coulter (Omnisorb 100 CX) instrument. The mesopore areas were obtained from the  $t$ -plots of the adsorption data at higher partial pressures.

The framework IR spectra of the samples were recorded in a Nicolet (60 SXB model) FTIR spectrometer using KBr pellets. XPS measurements were carried out in a VG Scientific ESCA-3-MK 2 electron spectrometer with Al K $\alpha$  X-ray source. A binding energy of 285 eV for C 1s level was used as internal standard.

<sup>29</sup>Si MAS-NMR spectra were recorded at 59.6 MHz on a Bruker MSL-300 NMR spectrometer. <sup>119</sup>Sn NMR spectra were obtained at 111.82 MHz. Typically around 3000 transients were signal averaged before Fourier transformation. The chemical shifts (in the case of Sn) were referenced externally to tetramethyltin.

### 2.3. Catalytic oxidation reactions

The catalytic runs were carried out batch wise. In a standard run for phenol hydroxylation using aqueous H<sub>2</sub>O<sub>2</sub> as oxidant, 10 g phenol, 1.0 g of the catalyst (particle size of 0.2 to 0.3  $\mu$ m) and 20 g H<sub>2</sub>O were placed in the reaction vessel. After the required temperature of 348 K was attained, 4.6 g H<sub>2</sub>O<sub>2</sub> (26% aqueous solution) was added through a feed pump. The product aliquots were taken out periodically for analysis in a capillary GC (HP 5880) fitted with a 50 m long silicon–gum column. For toluene oxidation, 200 mg of the catalyst was used for 10 g toluene and acetonitrile (20 g) was used as solvent. The conversions are given as mol-% of the substrate consumed at a given time and limited by the initial substrate to H<sub>2</sub>O<sub>2</sub> (mole) ratio of 3 in the reaction mixture.

## 3. Results and discussion

### 3.1. Crystallization, structure and morphology

The XRD profiles of the Sn-silicate samples match well with that of Sn-free silicalite-2 sample (Fig. 1). All these samples are highly crystalline and belong to tetragonal space group I4m2 [13]. These are free from any MFI impurity. In the XRD patterns, the lines at 2 $\theta$  = 9.05° and 24.05° (both these lines are characteristic

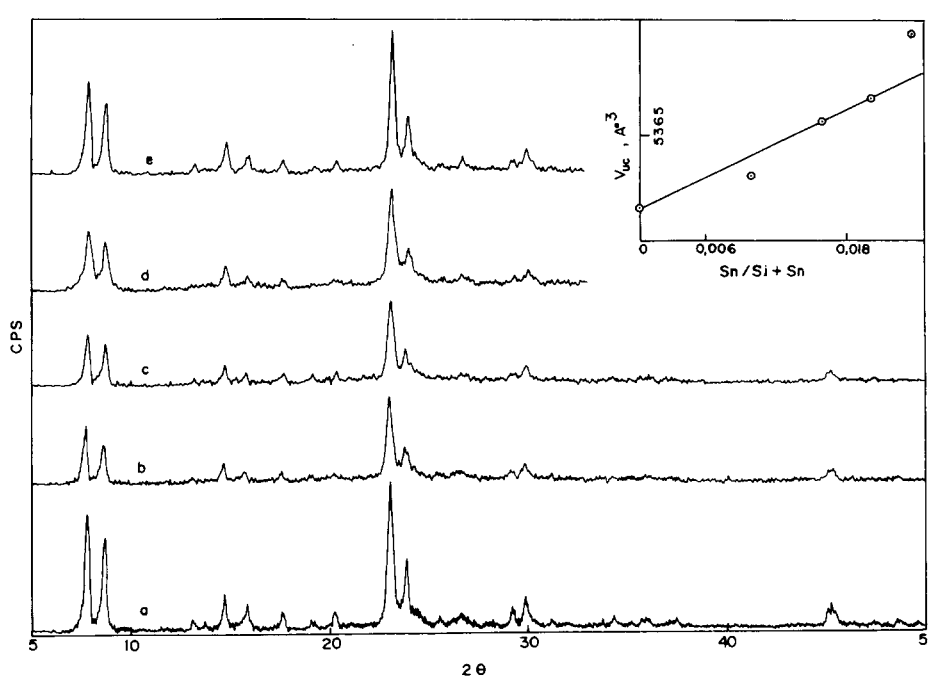


Fig. 1. XRD profiles of calcined silicalite-2 (MEL) sample (curve a) and Sn-silicalite samples prepared by hydrothermal synthesis with Si/Sn ratios of 40, 50, 70 and 100 (curves b to e, respectively). Inset: increase in the unit cell volume with Sn content in the samples.

of MFI structure) are absent. Further, a peak at  $2\theta = 45^\circ$  is present as a singlet. Compared to the XRD pattern of silicalite-2 sample, the Sn-silicate samples show somewhat broader peaks due to smaller crystallite size. Scanning electron micrographs of the samples (Fig. 2) indeed show that the crystalline particles are fairly uniform and of 3–5  $\mu\text{m}$  size in the case of Sil-2 and 0.2–0.5  $\mu\text{m}$  for all Sn-Sil-2 samples. No other impurity phases are visible.

During the crystallization, the uptake of tin into the silicalite network depends on the conditions of the preparation, particularly the pH of the gel which was 12.3. It is important that the reaction between  $\text{SnCl}_4$  and TEOS is complete before the addition of the organic base and that at such pH levels no hydroxide or oxyhydroxide of Sn is precipitated. The chemical analysis (Table 1) of the calcined, crystalline Sn-Sil-2 samples shows that the Si/Sn ratio is almost similar to that of the gel. During the synthesis of Sn-silicalite-1 (MFI) in fluoride medium (pH = 6.3), we noticed that very large crystals of silicalite-1 were formed, apparently with no Sn incorporation into the structure [14] (vide infra).

Table 1 shows the tetragonal unit cell volumes of the MEL-type Sn-silicates,  $V_{\text{uc}}$ , which increases with the number of Sn atoms in the sample (total Sn per unit cell) (Fig. 1, inset). If at least a part of the tin is located within the framework of the silicalite-2 structure, such an increase should take place (Shannon ionic radii, 0.55 Å for  $\text{Sn}^{4+}$  and 0.26 Å for  $\text{Si}^{4+}$ ). Based on a theoretical calculation of unit-cell volume expansion, we estimate that one fifth of the Sn atoms are probably in

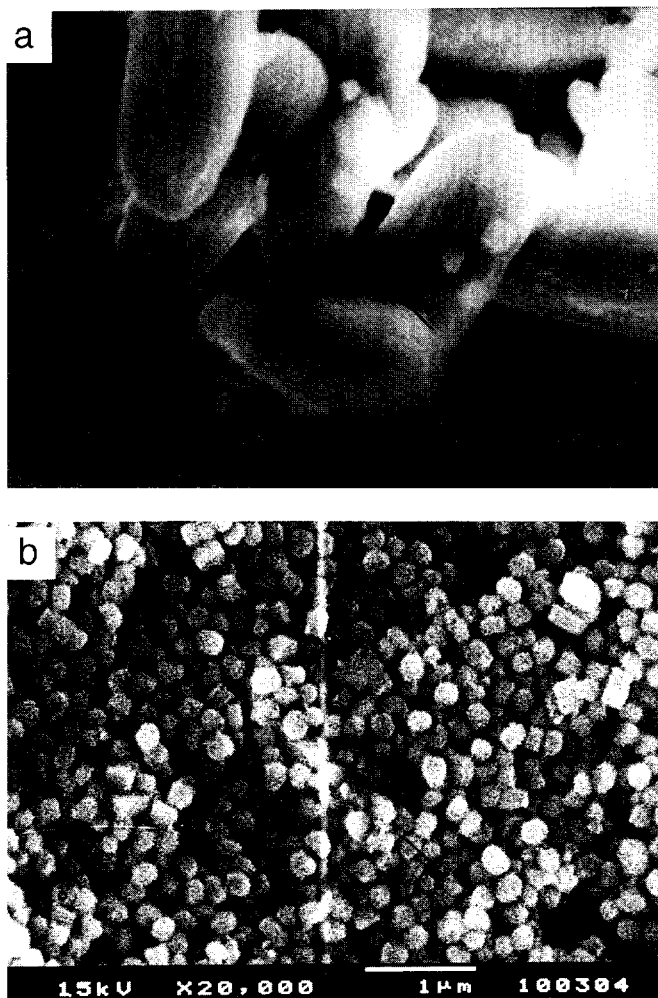


Fig. 2. Scanning electron micrographs of Sn-free silicalite-2 (a) and Sn-silicalite-2 sample with Si/Sn = 70 (b).

the framework positions in these samples. A similar observation was made with our Sn-silicate-1 (MFI) samples [12].

### 3.2. IR spectra

The framework IR spectra of three Sn-Sil-2 samples, the amorphous Sn-silica (gel) sample, Sn-impregnated Sil-2 and pure  $\text{SnO}_2$  are given in Fig. 3, curves, a–c, d, e and f, respectively. There is a clear shift of the wavenumber of the T–O–T lattice vibration ( $1110\text{ cm}^{-1}$ ) towards lower values with increasing tin content per unit cell of the Sn-Sil-2 samples. An analogous shift observed for other MFI-type metallosilicates has been attributed to heteroatom incorporation into the MFI framework [15,16]. In addition, we also observe a shoulder at around  $970\text{ cm}^{-1}$  in the IR spectra of Sn-Sil-2 samples (curves a–c) and amorphous Sn-silica (gel) sample

Table 1  
Composition and physico-chemical characteristics of Sn-silicalite-2 samples

Sample	Si/Sn (mole ratio)		$V_{uc}$ ( $\text{\AA}^3$ )	Sorption capacity <sup>a</sup> (wt.-%)			<sup>119</sup> Sn NMR <sup>b</sup> ( $\delta$ ppm)	Surface area ( $\text{m}^2$ $\text{g}^{-1}$ )	Mesopore area ( $\text{m}^2 \text{g}^{-1}$ )	Micropore volume ( $\text{ml g}^{-1}$ )	
	Gel	Product <sup>c</sup>		H <sub>2</sub> O	Cyclo- hexane	<i>n</i> - Hexane					
	Chem. anal.	XPS									
Sn-Sil-2	40	41	39	5370	9.0	11.5	14.2	–	532	39	0.21
Sn-Sil-2	50	49	44	5360	8.5	11.3	14.0	–739	557	30	0.21
Sn-Sil-2	70	63	65	5358	7.5	11.0	13.7	–705	554	35	0.25
Sn-Sil-2	100	102	98	5349	7.2	10.5	13.5	–740	506	56	0.18
Sn- Silica (gel) <sup>d</sup>	70	70	–	–	10.6	12.7	12.5	–	530	256	0.12
Sil-2 <sup>e</sup>	–	–	–	5345	4.0	8.0	12.4	–	387	7	0.15
Sn- impreg. Sil-2	50	50	–	–	8.6	4.0	9.8	–604	467	54	0.15

<sup>a</sup> Gravimetric (Cahn balance) adsorption at  $p/p_0=0.5$  and at 298 K.

<sup>b</sup> Chemical shift with respect to  $\text{Me}_4\text{Sn}$ .

<sup>c</sup> Calcined product. Bulk composition by chemical analysis and surface composition by XPS.

<sup>d</sup> Amorphous sample, for comparison (see Section 2).

<sup>e</sup> Sn-free silicalite (MEL structure) for comparison, prepared according to the procedure given in US patent 3 709 979 (1973).

(curve d). In silastannoxanes of the type,  $R_3\text{Sn-O-SiR}'_3$ , an intense IR band observed at  $950\text{--}980 \text{ cm}^{-1}$  is associated with asymmetric stretching vibration of the Si–O–Sn group [17]. A similar observation for Ti- and V-silicates with MFI and MEL structures has been attributed to Si–O–M vibrations from the possible substitution of heteroatom (*M*) in the Si–O–Si units [9,18]. In Sn-impregnated Sil-2 sample, no such vibration is noticed (curve e). Substitution of  $\text{Sn}^{4+}$  cation within the oxygen framework of MFI was not evidenced in an earlier study [19].

### 3.3. Texture and sorption characteristics

The  $\text{N}_2$  adsorption isotherms at 77 K of Sn-Sil-2 samples are characteristic of microporous materials. The adsorption isotherms presented in Fig. 4 show clearly the textural difference between the crystalline, microporous silicalite-2, Sn-impregnated silicalite-2 and Sn-Sil-2(70) on the one hand (curves a,b and d, respectively) and the amorphous Sn-silica (gel) (curve c) on the other. The surface areas are in the range of  $500 \text{ m}^2 \text{ g}^{-1}$  for all the Sn-samples as against a value of  $387 \text{ m}^2 \text{ g}^{-1}$  recorded for Sn-free Sil-2 sample (Table 1). Difference in the particle sizes and presence of more defect sites in Sn-Sil-2 samples may account for this variation. The meso-pore (t-area) contribution calculated from the adsorption isotherms at higher partial pressures is rather small in all Sn-Sil-2 samples. For the amorphous

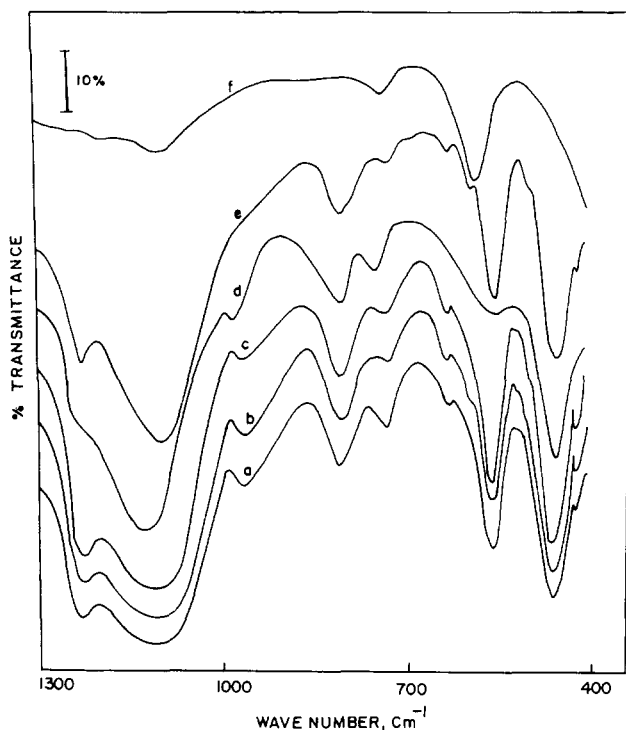


Fig. 3. Framework FT-IR spectra of Sn-Sil-2 samples with Si/Sn ratios of 50, 70 and 100 (curves a, b and c, respectively), amorphous Sn-silica (gel) (curve d), Sn-impregnated silicalite-2 (curve e) and SnO<sub>2</sub> (curve f).

Sn-silica (gel) sample, almost 50% of the surface area contribution comes from the mesopores (Table 1). Pure SnO<sub>2</sub> has a low surface area.

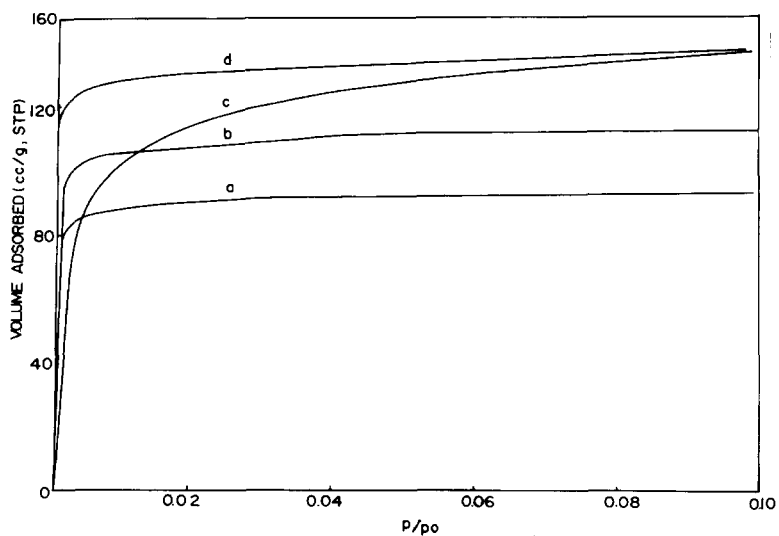


Fig. 4. N<sub>2</sub> adsorption isotherms at 77 K of silicalite-2 (curve a), Sn-impregnated silicalite-2 (curve b), amorphous Sn-silica (gel) (curve c) and crystalline Sn-Sil-2(70) sample (curve d).

One of the important properties of these microporous materials is their sorption characteristics. The micropore volumes are in the range of 0.15–0.25 ml g<sup>-1</sup> for all the samples. The amounts of H<sub>2</sub>O, n-hexane and cyclohexane adsorbed by these samples at 298 K and at  $p/p_0$  of 0.5 are included in Table 1. From the amount of H<sub>2</sub>O adsorbed, it may be concluded that incorporation of Sn into the silicalite-2 structure decreases the hydrophobicity of the samples. The comparable sorption capacities for n-hexane and cyclohexane between Sil-2 and Sn-Sil-2 samples indicate that the micropores (volumes) are maintained and that occluded SnO<sub>2</sub>-type of species may not be present in these samples. For the Sn-impregnated-Sil-2 sample, the sorption capacity for cyclohexane and n-hexane is somewhat lower.

### 3.4. XPS and surface composition

The X-ray photoelectron spectra of the samples showed typical doublets for Sn 3d<sub>3/2</sub> and 3d<sub>5/2</sub> electrons with the binding energies of 494.2 and 485.8 eV, respectively, confirming the presence of Sn in 4+ oxidation state on the surface. The surface chemical compositions were calculated from the integrated intensities of Sn 3d and Si 2s peaks, taking the values of photoionisation cross sections of the photoelectron kinetic energy reported by Scofield [20]. The surface Si/Sn ratios of the samples compare reasonably well with the bulk composition of the samples (Table 1) and confirm the presence of Sn<sup>4+</sup> in the bulk of the samples. Extraction with conc. HCl did not remove any tin from the samples, confirming the absence of Sn<sup>2+</sup> ions in our samples.

### 3.5. <sup>29</sup>Si and <sup>119</sup>Sn MAS-NMR spectra

The <sup>29</sup>Si NMR spectra (Fig. 5) of the as-synthesized samples exhibit an intense resonance at -112 ppm flanked by a low field signal at -104 ppm (with respect to Me<sub>4</sub>Si). Upon calcination, the intensity of the low field resonance is reduced. The broad high field resonance is due to the Si(OSi) environment, which in a material synthesized using fluoride medium (pH 6.3) [14] shows the expected 24-fold crystallographic multiplicity of monoclinic ZSM-5 lattice. The resonance at -104 ppm arises primarily from Si at the defect sites, containing SiOH, Si(OH)<sub>2</sub> and Si-O-R [21]. Si(1Sn) environment, even if present, is not detectable in the <sup>29</sup>Si NMR spectrum due to high Si/Sn ratio of the samples. Thus, <sup>29</sup>Si MAS-NMR indicates merely the presence of terminal silanol groups at which site tin is possibly located, as further evidenced by <sup>119</sup>Sn MAS-NMR. Despite the high Si/Sn ratio of the samples, <sup>119</sup>Sn NMR signals are detectable owing to large sensitivity associated with the spin 1/2 of <sup>119</sup>Sn nucleus. They also allow us to probe the tin environment directly. In order to get a benchmark on the observed <sup>119</sup>Sn chemical shifts, tin NMR spectra were also recorded for a TEOS + SnCl<sub>4</sub> complex and a Sn-silicalite-1 synthesized in fluoride medium [14]. The former gave a band of signals in the range, -622 to -675 ppm, with an intense resonance at -645 ppm. For the latter,

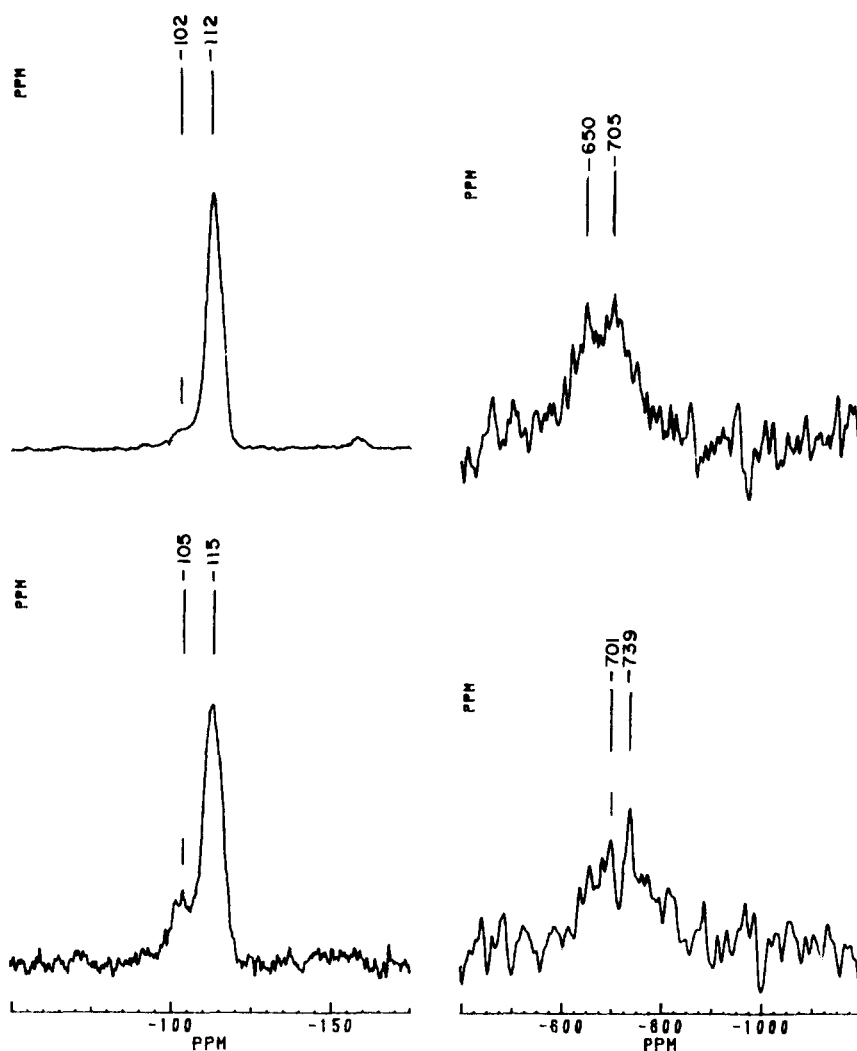


Fig. 5.  $^{29}\text{Si}$  MAS-NMR spectra of as-synthesized (bottom left) and calcined (top left) Sn-Sil-2(50) sample.  $^{119}\text{Sn}$  MAS-NMR spectra of calcined Sn-Sil-2(50) (bottom right) and Sn-Sil-2(70) (top right) samples.

a sharp resonance was observed at  $-604$  ppm. This matches well with the tin resonance in pure  $\text{SnO}_2$  [22]. For the as-synthesized and calcined Sn-Sil-2 samples, we were able to detect  $^{119}\text{Sn}$  resonance, although the signal to noise ratio was poor (Fig. 5). The  $^{119}\text{Sn}$  signal is located in the range,  $-700$  to  $-740$  ppm for all the samples (Table 1).

It may be noted that the octahedrally coordinated tin in pure  $\text{SnO}_2$  has a chemical shift of  $-604$  ppm. In many ternary tin oxides the octahedral tin environment resonates in the chemical shift range of  $-450$  to  $-700$  ppm [22]. For the octahedrally coordinated tin in the mineral sorensonite, a chemical shift value of  $-706$  ppm has been noted [21]. Thus, there is an approximately 300 ppm range for one particular type of coordination for  $\text{Sn}^{4+}$ , although the overall  $^{119}\text{Sn}$  chemical shift

Table 2  
Hydroxylation of phenol on Sn-silicalite-2 molecular sieves<sup>a</sup>

Sample	Phenol conv. <sup>b</sup> (mol-%)	H <sub>2</sub> O <sub>2</sub> Sel. <sup>c</sup> (mol-%)	Product distribution <sup>d</sup> (%)			
			CAT	HQ	PBQ	Tar
Sn-Sil-2(50)	20.0	63.1	52.1	42.4	0.3	5.2
Sn-Sil-2(70)	17.2	54.1	51.8	43.2	0.2	4.8
Sn-silica (gel) (70)	16.5	52.5	70.1	23.3	0.6	6.0
Sn-impreg.-Sil-2(50)	1.0	3.0	67.0	33.0	–	–
SnO <sub>2</sub>	0.5	1.5	65.0	35.0	–	–

<sup>a</sup> Reaction conditions: catalyst/phenol = 10 g mol<sup>-1</sup>; solvent (water) = 20 g; phenol/H<sub>2</sub>O<sub>2</sub> (mole) = 3; temp. = 348 K; reaction time = 24 h; addition of H<sub>2</sub>O<sub>2</sub> in one lot.

<sup>b</sup> Mol consumed for the formation all products per mol initially taken × 100.

<sup>c</sup> H<sub>2</sub>O<sub>2</sub> consumed (mol-%) for the formation of all products.

<sup>d</sup> Break up (mol-%) of the products catechol (CAT), hydroquinone (HQ) and para-benzoquinone (PBQ) including tar.

<sup>e</sup> For similar amount of Sn as in the case of Sn-Sil-2(50).

range spans several thousand ppm [23]. The observed chemical shifts for the as-synthesized and calcined materials are in overlap with the reported range for octahedral tin. In view of the much broader <sup>119</sup>Sn resonance observed in these samples, we can ascribe tin to be octahedrally coordinated. It is then more probable to think of tin incorporation at or very close to the defect sites than of a tetrahedral substitution in the lattice. This conclusion is consistent with the observation that in the material synthesized under fluoride medium, there are practically negligible defect sites and the <sup>119</sup>Sn MAS-NMR is identical to that of SnO<sub>2</sub> [14].

### 3.6. Catalytic activity

Interestingly, these Sn-silicates are catalytically active in the hydroxylation reactions with aqueous H<sub>2</sub>O<sub>2</sub> [12]. The hydroxylation of phenol and the oxidation of toluene are performed over two of the Sn-Sil-2 samples (Si/Sn = 50 and 70) under one set of conditions. For comparison, blank reactions were carried out on pure SnO<sub>2</sub> and a Sn-impregnated silicalite-2 sample. The results (Tables 2 and 3) show that whereas SnO<sub>2</sub> and the Sn-impregnated silicalite-2 samples have negligible activity, the Sn-Sil-2 samples show fairly good activity in these hydroxylation reactions. In the hydroxylation of phenol, the conversions on the two samples range from 17 to 20 mol-% with H<sub>2</sub>O<sub>2</sub> selectivity of 54 to 63 mol-% (Table 2). Under similar conditions, the phenol conversions are 20 and 25 mol-% over Sn-silicate-1 (MFI) and TS-1 samples, respectively, with H<sub>2</sub>O<sub>2</sub> selectivity of over 65 mol-% [12]. For comparison, we have included the results on the catalytic activity of the amorphous Sn-silica prepared from the gel (see Experimental). A phenol conversion of 16.5 mol-% which is comparable to that with Sn-Sil-2(70) sample indicates that well-dispersed Sn<sup>4+</sup> ions present in both the amorphous and crystalline Sn-samples are responsible for the catalytic activity. However, significant difference

Table 3  
Oxidation of toluene on Sn-silicalite-2 molecular sieves<sup>a</sup>

Sample	Toluene conv. <sup>b</sup> (mol-%)	H <sub>2</sub> O <sub>2</sub> sel. <sup>c</sup> (mol-%)	Product distribution <sup>d</sup> (%)					
			<i>o</i> -Cresol	<i>p</i> -Cresol	<i>m</i> -Cresol	Benzyl alcohol	Benzaldehyde	Others
Sn-Sil-2(50)	7.6	45.2	5.0	8.2	1.6	10.2	72.2	2.8
Sn-Sil-2(70)	7.2	43.1	4.1	8.8	1.2	11.5	71.4	3.0
Sn-Silica(gel)(70)	5.0	18.3	8.0	29.0	0.5	32.3	26.0	4.2
Sn-impreg.-Sil-2(50)	0.5	1.5	nd <sup>e</sup>	70.0	nd	nd	nd	30.0
SnO <sub>2</sub>	0.0	–	–	–	–	–	–	–

<sup>a</sup> Reaction conditions: catalyst/toluene = 20 gmol<sup>-1</sup>; solvent (acetonitrile) = 20 g; toluene/H<sub>2</sub>O<sub>2</sub> (mol) = 3; temp. = 353 K; reaction time = 24 h.

<sup>b</sup> Toluene consumed (mol-%) in the formation of all products.

<sup>c</sup> H<sub>2</sub>O<sub>2</sub> consumed (mol-%) in the formation of cresols, benzyl alcohol and benzaldehyde.

<sup>d</sup> Break up (mol-%) of products.

<sup>e</sup> Not detected.

<sup>f</sup> For similar amount of Sn as in the case of Sn-Sil-2(50).

in the product distribution between these two samples is noticed (Table 2). In the product distribution, a catechol to hydroquinone ratio of 1.2 for the two crystalline Sn-Sil-2 samples indicates a certain degree of shape selectivity which is not observed with amorphous Sn-silicate (gel) sample. It may be noted that a catechol to hydroquinone ratio of 0.9 to 1.1 has been reported for the titanium silicalites (TS-1 and TS-2) earlier [24]. These results indicate that in addition to being well-dispersed, the Sn<sup>4+</sup> ions are probably located within the channels of the MEL structure in the Sn-Sil-2 samples.

Table 3 compares our results on the oxidation of toluene over the Sn-samples. Both SnO<sub>2</sub> and Sn-impregnated Sil-2 samples show negligible activity. The Sn-Sil-2 samples are active in this reaction (7.2 to 7.6 mol-% conversion of toluene in 24 h) and catalyze the hydroxylation of the aromatic molecules to give essentially *o*- and *p*-cresols (more para selective) as well as the oxidation of the methyl substituent to give benzyl alcohol and benzaldehyde in the product. In this respect the Sn-silicate molecular sieves appear to be similar to the vanadium silicalites (VS-2) [25]. Even though the amorphous Sn-silica (gel) is also active, the H<sub>2</sub>O<sub>2</sub> selectivity is poor. From the product distribution, it is seen that the side chain oxidation is more extensive with Sn-Sil-2 samples than with the amorphous Sn-silica. Presumably, the reason for the catalytic oxidative activity of the Sn-silicates is due to the reduction of isolated Sn<sup>4+</sup> to Sn<sup>2+</sup>, the Sn<sup>2+</sup> being oxidised back with H<sub>2</sub>O<sub>2</sub>, but further detailed studies are required before possible mechanisms of oxidation could be discussed. These Sn-silicate molecular sieves are thermally stable and can be regenerated after the reaction without significant loss of catalytic activity.

#### 4. Conclusions

Sn-silicalite molecular sieves (Si/Sn molar ratios > 40) synthesized under hydrothermal conditions are very similar both structurally and texturally to silicalite-2 (MEL type) material, with a part of the Sn<sup>4+</sup> ions probably in the framework positions. The formation of Si–O–Sn linkage is indicated in the framework IR spectra of the samples. The MAS-NMR studies indicate that most of the Sn species are octahedrally coordinated and that they are probably linked to the silicalite structure through defect sites. These are active in the hydroxylation/oxidation reactions. The hydroxylation of phenol and toluene with aqueous H<sub>2</sub>O<sub>2</sub> is catalyzed by isolated Sn species. The observed product shape selectivity indicates that the active Sn species are located within the channels of the MEL structure.

#### Acknowledgements

We thank Dr. S. Badrinarayanan for XPS spectra and Dr. A.A. Belhekar for the IR spectra of the samples. One of us (NKM) is grateful to CSIR, New Delhi for a research fellowship.

#### References

- [1] G.W. Skeels and E.M. Flanigen, *Stud. Surf. Sci. Catal.*, 49A (1989) 331.
- [2] G.W. Skeels and E.M. Flanigen, US Patent Appl. 133 372 (1987).
- [3] G.W. Skeels and E.M. Flanigen, EP 321 177 (1989).
- [4] D.E.W. Vaughan and S.B. Rice, US Patent 4 933 161 (1990) assigned to Exxon.
- [5] F.G. Dwyer and E.E. Jenkins, US Patent, 3 941 871 (1976) assigned to Mobil.
- [6] E.W. Corcoran, Jr. and D.E.W. Vaughan, US Patent, 5 192 519 (1993) assigned to Exxon.
- [7] I.G.K. Andersen, E.K. Andersen, N. Knudsen and E. Skou, *Solid State Ionics*, 46 (1991) 89.
- [8] N. Knudsen, E.K. Andersen, I.G.K. Andersen and E. Skou, *Solid State Ionics*, 35 (1989) 51.
- [9] N.J. Tapp and C.M. Cardile, *Zeolites*, 10 (1990) 680.
- [10] G. Perego, G. Bellusi, C. Corno, M. Taramasso, F. Buonomo and A. Esposito, *Stud. Surf. Sci. Catal.*, 28 (1986) 129.
- [11] Z. Gabelica and J.L. Guth, *Stud. Surf. Sci. Catal.*, 49A (1989) 421.
- [12] Naval Kishor Mal, Veda Ramaswamy, S. Ganapathy and A.V. Ramaswamy, *J. Chem. Soc., Chem. Commun.*, (1994) 1933.
- [13] C.A. Fyfe, H. Gies, G.T. Kokotailo, C. Pasztor, H. Strobl and D.E. Cox, *J. Am. Chem. Soc.*, 111 (1989) 2470.
- [14] Naval Kishor Mal and A.V. Ramaswamy, unpublished results.
- [15] R. Szostak, *Molecular Sieves: Principles of Synthesis and Identification*, Van Nostrand Reinhold, New York, 1989.
- [16] G. Vorbeck, J. Janchen, B. Parlitz, M. Schneider and R. Fricke, *J. Chem. Soc., Chem. Commun.*, (1994) 123.
- [17] H. Schmidbauer, *Angew. Chem. Int. Ed.*, 4 (1965) 201.
- [18] P.R. Hari Prasad Rao, A. V. Ramaswamy and P. Ratnasamy, *J. Catal.*, 137 (1992) 225.
- [19] V. Valtchev, *God. Sofii Univ. Sv. Kliment Okhridski, Geol.-Geogr. Fak.* 83 (1992) 87 (Bulg.), CA 120: 40697k.
- [20] J.H. Scofield, *J. Elect. Spect. Relat. Phenom.*, 8 (1976) 129.

- [21] A. Sebald, L.H. Merwin, W.A. Dollase and F. Seifert, *Phys. Chem. Min.*, 17 (1990) 9.
- [22] N.J. Clayden, C.M. Dobson and A. Fern, *J. Chem. Soc. Dalton Trans.*, (1989) 843.
- [23] B. Wrackmeyer, *Ann. Rep. NMR Spectroscopy*, 16 (1985) 73.
- [24] P.R. Hari Prasad Rao and A.V. Ramaswamy, *Appl. Catal. A*, 93 (1993) 123.
- [25] A.V. Ramaswamy and S. Sivasanker, *Catal. Lett.*, 22 (1993) 239.